Direct Non-invasive MRI Measurement of the Absolute CBV-CBF Relationship during Visual Stimulation in Normal Humans

Pelin Aksit Ciris[1], Maolin Qiu[1], and Robert Todd Constable[1]
[1]*Yale University, New Haven, CT, United States*

Introduction: BOLD fMRI is a powerful noninvasive approach for studying brain physiology with high sensitivity, however, signal reflects physiologic alterations including changes in CBV, CBF, blood oxygenation and metabolism (1-4), and physiological interpretation is limited. While methods exist for non-invasive absolute CBF quantification, most calibrated fMRI studies typically assume $CBV=0.88CBF^{0.38}$ based on the absolute CBV-CBF relationship obtained in monkey brains under hypo/hypercapnia using PET (5). This practice is controversial since this relation may vary across brain regions, functional challenges, and species, as demonstrated by published power parameters ranging from 0.18-0.64 in steady-state across species, stimuli, modalities, relative and absolute contributions of whole/partial blood compartments (6-16). This study presents MRI measurement of the absolute CBV-CBF relationship in humans, which has not been available mainly since CBV measurement has been invasive and difficult especially in human subjects.

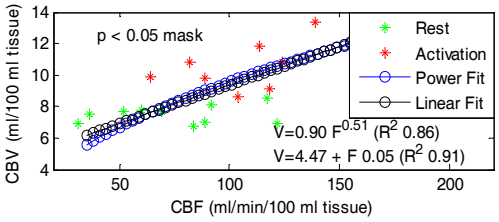

Methods: Twelve normal volunteers participated in this IRB-approved study. Absolute CBV was quantified non-invasively using a method based on acquisitions with varying extents of blood nulling at rest and activation, and fitting of signal changes to a three-compartment biophysical model (17-19); all volunteers were imaged with a recently developed extension of this method which enables whole-brain multi-slice imaging through a rotating slice acquisition and maintenance of steady state throughout varying inversion and recovery durations (19). Absolute CBF was quantified in ten volunteers using Q2TIPS PASL (20). Data was acquired at 3T (Tim Trio, Siemens, Erlangen, Germany) using a 32 channel head coil. High-resolution 3D, and 2D T1w images at same slice locations as CBV and CBF were used for registration. CBV and CBF were acquired during flashing checkerboard visual stimulation (3 OFF/ON cycles, 78s each, 10Hz) consecutively with 20 transverse slices covering the whole brain and: 192x256mm FOV, 4x4x4mm, GE EPI, CBV parameters: TE/TS/TR:11ms/1.2s/3s, 60 TIs:400-1158ms, 3 averages. CBF parameters were TE/TI1/ TR/sliceTR:20ms/1.4s/3s/52.3ms, 10cm adiabatic inversion 2cm inferior/superior, and bipolar gradient of 5cm/sec; PD with CBF parameters except TR/TI/TD=8s/6.05s/0. GM CBV data was calculated in MNI space allowing 18sec of each stimulus transition for settling of the hemodynamic response and averaging over blocks. CBV and CBF data was motion and drift corrected, and smoothed with an 8mm Gaussian kernel. CBF data was processed in each subjects' space, then registered to MNI space. Voxels with CBV>30ml/100g were excluded as vessels. Activation masks were generated from regions with significant differences between CBV values at rest vs. activation, and CBF values at rest vs. activation, with $p<0.01$, $p<0.05$, and $p<0.1$. Results are reported from the intersection of CBV and CBF activation masks within Brodmann areas 17 and 18. The CBV-CBF relationship is reported from the mean of two approaches: averaging data over mask regions, such that data is condensed to one rest and one activation value for each volunteer, followed by fitting to this mask-averaged volunteer data (i.e. Fig1); and fitting at each voxel across volunteers' rest and activation data (where a minimum of three points exist), followed by averaging fitting results (with $r^2 > 0.9$) over mask regions (i.e.Fig2). Median was used in averaging across masks for exclusion of outliers. All data was processed with both a power fit ($V = a F^{b}$) and a linear fit ($V = c + F d$), using each of the three activation level masks.

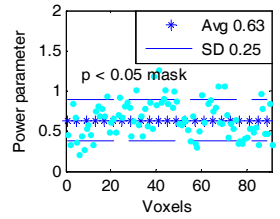

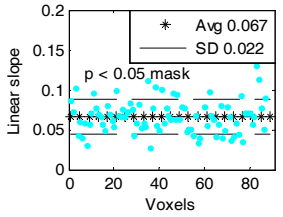

Results and Discussion: The stimulus resulted in bilateral CBV and CBF increases in occipital lobes of all volunteers. Factors that could influence vascular parameters were not matched across volunteers to obtain data across a wide range of values for fitting across rest and activation conditions. Averaged ranges over activation masks for CBV were 7.4±0.6, 10.7±1.8, and 8.8±2.2 ml/100ml at rest, activation, and over both conditions, respectively; in close agreement with occipital cortical GM CBV reported as 7±1.12ml/100ml using bolus tracking (21). iVASO methods reported resting GM arterial CBVs of 2.04±0.27, 0.76±0.17ml/100 ml (22); and 1.6ml/100ml (23). Considering 21% arterial contribution in baseline CBV (24,4), our resting CBV results correspond to an arterial CBV of 1.55ml/100ml, well within the range of iVASO results. Changes in CBV during visual activation in humans have previously been reported as 18.2% (25) and 27% (26) with bolus tracking; 32% (17) and 31% (18) with the biophysical model; 56% with multi-echo VASO (27); and 68% with PET (6). A comparable increase of 44.6% was observed in this study. More pronounced inter-subject variability was observed in CBF with two of the youngest three female volunteers influencing CBF statistics as follows: 76±30, 119±40, 92±42 ml/min/100ml at rest, activation, and over both conditions, respectively, over all volunteers; or 65±22, 110±24, 84±31 ml/min/100ml for CBF at rest, activation, and over both conditions, respectively, excluding two volunteers, which is in close agreement with baseline PET results of 65.1 ml/min/100 ml (12), and the 57% increase observed across all volunteers is in agreement with the 55% increase with PASL during high intensity visual stimulation (15). Fits on all masks are summarized in Table 1, Figures demonstrate results for $p < 0.05$. CBV vs. CBF is shown in Figure 1 using the volunteer based approach: fitting to a power function resulted in the expression $V = 0.90 F^{0.51}$ in very reasonable agreement with Grubb's original relationship of $V = 0.88 F^{0.38}$ (5); fitting to a linear function resulted in a slightly improved fit with $V = 4.47 + F 0.05$. Power and slope parameters from fitting individual voxels are shown in Figure 2 along with their mean and one standard-deviation range: the linear slope values have a smaller relative standard-deviation, and the power parameter of 0.63±0.25 is in excellent agreement with PET measurements in cortical GM of 0.64±0.26 (15). The CBV-CBF relationship was generated in Figure 3 using the mean power and linear fit results (dotted and dashed lines are one standard-deviation changes in the first and second parameter of each fitting method, respectively); power and linear fits overlap significantly, and once again linear fitting has relatively smaller standard deviation.

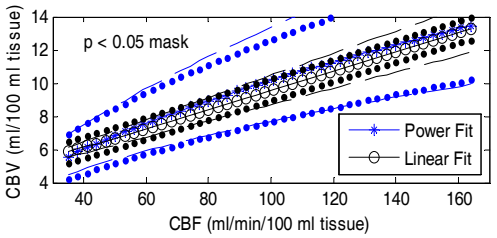

Table1	Power Fit: $V = a F^{b}$		Linear Fit: $V = c + F d$	
Mask	a	b	c	d
$p < 0.01$	0.56±0.03	0.61±0.01	3.46±0.07	0.057±0.001
$p < 0.05$	0.73±0.18	0.57±0.06	3.81±0.66	0.058±0.009
$p < 0.10$	0.71±0.23	0.58±0.08	3.65±0.77	0.058±0.009

Conclusion: Direct non-invasive MRI measurement of the absolute CBV-CBF relationship was presented in normal humans subjects. Measurements were within physiologically expected ranges, consistent with prior publications especially PET and contrast enhanced measurements in cortical GM, consistent with the exclusion of WM voxels in this study. Improved characterization of the CBV-CBF relationship in humans under various metabolic or functional challenges can form a solid basis for understanding of fMRI signal mechanisms and the relationship between neuronal activity, hemodynamic changes and metabolism leading to the BOLD effect, with further potential clinical utility in evaluating alterations of vascular state, characterizing damage, identifying disease and monitoring treatments or drug effects.

References: [1] Ogawa Biophys 1993;64 [2] Boxerman MRM 1995;34 [3] Buxton MRM 1998;39 [4] vanZijl NatMed 1998;4 [5] Grubb Stroke 1974;5 [6] Ito JCBFM 2001;21 [7] Jones Neuroimage 2001;13 [8] Lee MRM 2001;45 [9] Jones Neuroimage 2002;15 [10] Ito JCBFM 2003;23 [11] Wu MRM 2002;48 [12] Rostrup Neuroimage 2005;24 [13] Kida JCBFM 2007;27 [14] Jin Neuroimage 2008;43 [15] Chen NmrBiomed 2009;22 [16] Chen Neuroimage 2010;53 [17] Gu Neuroimage 2006;30 [18] Glielmi MRM 2009;61 [19] Ciris Ismrm 2011. [20] Luh MRM 1999;41 [21] Grandin Neuroimage 2005;26 [22] Hua NmrBiomed 2011 [23] Donahue JCBFM 2010;30 [24] Sharan AnnBme 1989;17 [25] Li Neuroimage 2000;12 [26] Francis MRM 2003;50 [27] Lu MRM 2005;53.